Journal of Magnetic Resonance 195 (2008) 112–115

Contents lists available at ScienceDirect

Journal of Magnetic Resonance

journal homepage: www.elsevier.com/locate/jmr

Communication

^{23}Na TQF NMR imaging for the study of spinal disc tissue

Kristopher J. Ooms [a], Marco Cannella [b], Alexander J. Vega [a,*], Michele Marcolongo [b], Tatyana Polenova [a,*]

[a] Department of Chemistry and Biochemistry, University of Delaware, 036 Brown Laboratories, Newark, 19716 DE, USA
[b] Department of Materials Science and Engineering, Drexel University, LeBow 27-444, 3141 Chestnut Street, Philadelphia, 19104 PA, USA

ARTICLE INFO

Article history:
Received 11 June 2008
Revised 25 July 2008
Available online 7 August 2008

Keywords:
Triple-quantum-filtered
^{23}Na NMR
Spinal disc
Imaging
PITQF

ABSTRACT

A method for acquiring triple quantum filtered (TQF) ^{23}Na NMR images is proposed that takes advantage of the differences in transverse relaxation rates of sodium to achieve positive intensity, PI, NMR signal. This PITQF imaging sequence has been used to obtain spatially resolved one-dimensional images as a function of the TQF creation time, τ, for two human spinal disc samples. From the images the different parts of the tissue, nucleus pulposus and annulus fibrosus, can be clearly distinguished based on their signal intensity and creation time profiles. These results establish the feasibility of ^{23}Na TQF imaging and demonstrate that this method should be applicable for studying human disc tissues as well as spinal disc degeneration.

1. Introduction

Degenerative disc disease of the spine causing lower back pain is one of the leading musculoskeletal disorders. According to various estimates, 15–20% of the population experiences lower back pain annually, and 60% or more over a lifetime [1]. While T_2 MRI is the most revealing non-invasive diagnostic technique for identifying changes in the disc anatomy, it has not been able to delineate symptomatic discs [2,3]. Other non-invasive methods are required in order to accurately diagnose disc degeneration so that the best course of treatment can be assigned without resorting to invasive techniques such as discography [4].

Numerous researchers have demonstrated that multiple-quantum-filtered, MQF, techniques can be used to study tissue samples [5–11]. Double-quantum-filtered, DQF, measurements of ^{1}H, ^{2}H, and ^{23}Na are the most common in biological tissues [12–14]. ^{1}H DQF relies on the dipolar coupling between protons to build-up double quantum coherence signal during the experimental creation time, τ [14]. Given the favorable NMR properties of ^{1}H, this may appear to be the most likely nucleus for study; however, it has been shown in our previous work that in some biological samples, such as spinal disc tissue, the residual dipolar couplings are too small to result in significant DQF signal [8]. Because of this we originally turned to ^{2}H DQF NMR spectroscopy which relies on the residual quadrupolar coupling to create double quantum coherence signal [8]. The major drawback in this approach is that the sample must be dialyzed to introduce significant amounts of $^{2}H_2O$ into the tissue. This is clearly not an ideal situation for samples that may change during dialysis or for *in vivo* studies. ^{23}Na NMR appears to be the logical choice then for studying biological tissues for which the sodium concentration under physiological conditions is high [15–17]. Indeed, in many cartilage-type tissues, the concentration is high because Na^+ provides a charge balance for the negative charge on the glycosaminoglycans which are a major component of the tissues. This is the case in human spinal disc tissues where concentrations of sodium ions are as high as 300 mM in healthy tissues [3,18,19].

We have recently shown that ^{23}Na DQF spectroscopy of human spinal disc tissue is sensitive both to the anatomy of the disc tissue, i.e. the nucleus pulposus or the annulus fibrosus, as well as the degenerative grade of the disc tissue [15]. The signal intensity build-up curves as a function of the DQF creation time, τ, showed trends that suggested this technique may be useful as a contrast mechanism for ^{23}Na magnetic resonance imaging. These experiments potentially provide a way of accessing information about both local order and dynamics as opposed to other methods proposed recently which provide a measure of relative ^{23}Na concentration in isotropic and anisotropic environments [16]. In order to extend the application of ^{23}Na MQF from a spectroscopic technique to an imaging method it is desirable to maximize the multiple-quantum signal. Previously it has been shown that by applying a triple quantum filter, TQF, instead of a double quantum filter, greater ^{23}Na signal intensity can be obtained while maintaining a similar τ-dependence of the NMR signal [20,21]. Fig. 1 demonstrates the increased signal obtained from the TQF experiment. The spectra in Fig. 1 are from a portion of human disc tissue obtained from a 67-year-old cadaver. The portion of the tissue in the NMR coil corresponds to the annulus fibrosus of the disc (the

* Corresponding authors.
E-mail addresses: lexvega@comcast.net (A.J. Vega), tpolenov@mail.chem.udel.edu (T. Polenova).

1090-7807/$ - see front matter © 2008 Elsevier Inc. All rights reserved.
doi:10.1016/j.jmr.2008.07.024

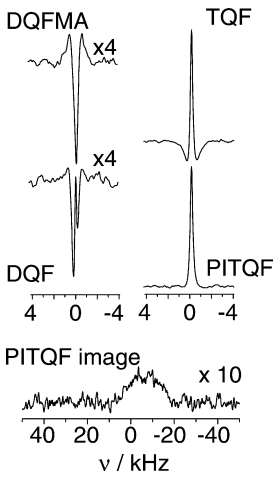

Fig. 1. Comparison of the ^{23}Na NMR spectra obtained using different MQF sequences. All spectra were processed with 200 Hz exponential line broadening except the PITQF image for which 500 Hz broadening was used. A 10.7 kHz/cm z-gradient was applied during the acquisition time of the PITQF image. The high frequency edge of the lineshape represents the edge of the sample while the low frequency edge marks the effective edge of the RF coil. Each spectrum is the sum of 512 scans using a 0.1 s pulse delay, τ = 1 ms, and t_{PI} = 0.5 ms.

same sample was used below for imaging experiments). All spectra were obtained with a 1 ms creation time. The signals obtained from the DQF and DQFMA are much less intense than that obtained from the TQF experiment.

One drawback in performing DQF or TQF imaging experiments on spin $I = 3/2$ nuclei such as ^{23}Na is that the lineshapes are composed of both positive and negative intensity signals with an overall integrated signal intensity near zero. In the case of TQF the positive intensity signal arises from the central NMR transition, i.e. $m_I = 1/2 \leftrightarrow -1/2$, while the negative lobes correspond to the two satellite transitions, $m_I = \pm 3/2 \leftrightarrow \pm 1/2$. When an imaging experiment is performed and the MQF signal intensity is spread out in the spatial dimension by the applied gradients, these components cancel each other out resulting in minimal signal being observed. A similar problem exists for ^{2}H DQF imaging due to the fact that the two transitions, $m_I = \pm 1 \leftrightarrow 0$, yield out-of-phase signals. To overcome this problem for ^{2}H, a modified DQF pulse sequence was developed which makes use of a z-filter to create in-phase DQF spectra for ^{2}H; this IPDQF sequence also works for ^{1}H [14,22–24].

For spin-3/2 nuclei, it is difficult to obtain in-phase signal by manipulating the spins using pulses without significant loss in the overall NMR signal intensity. In the frequency domain, the signal obtained from the third rank tensor components in a TQF pulse experiment have the form [5,20]:

$$\begin{aligned} S_{TQF}(\tau,\omega_2,\theta,\phi) &= -\frac{9\sqrt{2}}{80}(e^{-\tau/T_{2s}} - e^{-\tau/T_{2f}}\cos(\omega_Q\tau))(S_0 - S_1) \\ S_0 &= \frac{T_{2s}}{1+(\omega_2 T_{2s})^2} \\ S_1 &= \frac{1}{2}\left\{\frac{T_{2f}}{1+[(\omega_2+\omega_Q)T_{2f}]^2} + \frac{T_{2f}}{1+[(\omega_2-\omega_Q)T_{2f}]^2}\right\} \end{aligned} \quad (1)$$

where ω_Q is the quadrupole frequency. The two parts of the equation yield the signal intensity, $(e^{-\tau/T_{2s}} - e^{-\tau/T_{2f}}\cos(\omega_Q\tau))$, and the lineshape, $(S_0 - S_1)$. For Na^+ in an anisotropic environment, i.e., the ^{23}Na possessing a residual quadrupolar coupling, both the signal intensity build-up curves as a function of τ and the line shapes contain information about the bi-exponential T_2 relaxation, T_{2s} and T_{2f}, and the quadrupolar frequency, ω_Q. Previously, the full equations for DQF and DQFMA lineshapes were used to obtain accurate values of the three parameters of interest [15]. However, each component of Eq. (1) theoretically contains all the information needed. As mentioned, the challenge in applying TQF to imaging is in the lineshape of the TQF spectrum, the second part of the equation. It would be desirable to create a lineshape that is all positive in intensity, while maintaining the τ-dependence of the signal intensity. One simple way to achieve this is to take advantage of the difference in the two decay rates for the FIDs of the central and satellite transitions. The decay rate of the central transition is determined by the relatively long T_{2s}. The characteristic decay time, T_{2f}^*, of the satellite signal is determined by the combined effect of the faster relaxation time T_{2f} and the width of the Fourier transformed spectrum, which is given by the residual quadrupole coupling constant. In most of the tissue samples studied the two decay times are significantly different with T_{2s} values being as high as 20 ms, T_{2f} values typically being less than 4 ms, and satellite linewidths usually larger than 500 Hz, corresponding to decay T_{2f}^* values less than 1 ms [5,15,25]. By placing an additional delay, t_{PI}, in the pulse sequence after the TQF filter pulses, we can take advantage of the difference of the decay rates, see Fig. 2. Since T_{2f}^* is typically smaller than T_{2s}, we can choose an intermediate value for t_{PI} to ensure that the negative intensity signal from the satellites has decayed before data acquisition begins. The result is that only the central transition signal is observed, producing a sharp positive intensity peak that still possesses the τ dependence of the TQF experiment. This method, which we call positive intensity TQF (PITQF) was used to acquire the fourth spectrum shown in Fig.1. The PITQF experiment required a small number of optimization steps in order to set the optimal t_{PI}, which we checked for a number of τ values. The t_{PI} used in the spectrum displayed was 0.5 ms, a sufficiently long delay to achieve nearly complete decay of the FID corresponding to the wider-than-1 kHz satellite signal component at τ = 1 ms. For the sample studied, the spectrum shown in Fig. 1 illustrates that little signal from the central transition is lost and the PITQF is of similar intensity to the standard TQF experiment. The signal intensity as a function of τ behaves similarly to the central transition peak in both the DQF and TQF experiments and therefore can be interpreted in the same manner, providing information about the T_{2s} T_{2f} and ω_Q which can be related to the exchange dynamics and local order the sodium experiences. The success of the PITQF sequence will depend on the difference between T_{2f}^* and T_{2s} and will not work for samples where these two relaxation times are similar. However, for spinal disc tissues the technique should be generally applicable since in most cases these relaxation times are quite different.

With a purely positive intensity TQF NMR signal, it becomes possible to do imaging experiments. The final spectrum in Fig. 1 shows the 1D spatially resolved spectrum when a z-gradient was applied to the sample (gradient strength 10.7 kHz/cm). The high frequency side of the pattern is defined by the edge of the sample, while the low frequency side is determined by the edge of the RF

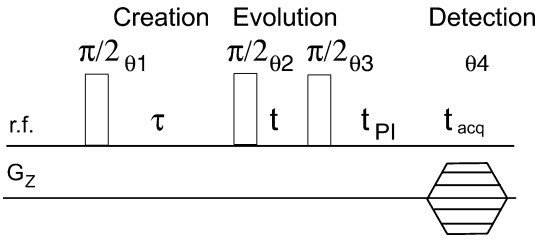

Fig. 2. The basic PITQF imaging sequence for 1D spatial resolution of the TQF NMR signal for spin $I = 3/2$. A π pulse can be inserted during τ for off-resonance acquisition and to refocus chemical shift and susceptibility broadening while phase encode gradients can be added during time t to spatially encode the x and y dimensions. The phase cycling is $\theta 1$ = 30, 90, 150, 210, 270, 330; $\theta 2$ = 120, 180, 240, 300, 360, 60; $\theta 3$ = 0; $\theta 4$ = 0, 180.

coil. This spectrum clearly demonstrates the feasibility of PITQF imaging.

To demonstrate how the PITQF experiment would work for analysis of spinal disc tissues we have obtained samples from two cadaveric spines with degenerative grades of 2 and 3, [26] ages 67 and 63. Rectangular cores were sampled from the side of the disc and placed inside 5 mm quartz NMR tubes. The sample placement was such that the annulus fibrosus part of the tissue was at the bottom of the tube, see Fig. 3. 1D images were acquired by applying a z-gradient on the broad-band solution NMR probe. Due to the RF coil size, the images were acquired in three steps by moving the sample through the coil and then summed together to form the full spectral profile. 1D images were taken as a function of the TQF creation time, τ, using a t_{PI} = 1.5 ms to ensure that only the central transition was observed even at lower τ values where the negative signal from the satellites is most intense, see Fig. 3. This procedure generates spectroscopic τ-images. As was demonstrated previously using ^{1}H DQF by Navon, Eliav and coworkers, [12,27,28] images as a function of τ can be useful indicators of the state of the cartilage tissues and have potential diagnostic value [27,28].

Based on previous studies it is known that the ^{23}Na MQF NMR build-up curves for healthy disc tissue show significantly different profiles for annulus fibrosus and nucleus pulposus. In a grade 1, 15-year-old sample it was found that the DQF creation time for maximum signal intensity of the nucleus was around 3 ms (90% of maximum signal reached after 1 ms) while the build-up and decay times for the nucleus pulposus were much longer (~90% of maximum signal occurred at 7–13 ms) [15]. Furthermore, the DQF signal intensity from the annulus was nearly three times stronger than that from the nucleus. The creation times of the DQF and PITQF signals should be comparable with the possible exception that at low τ values the relative signal intensity may be higher due to the lack of the negative intensity satellite peaks.

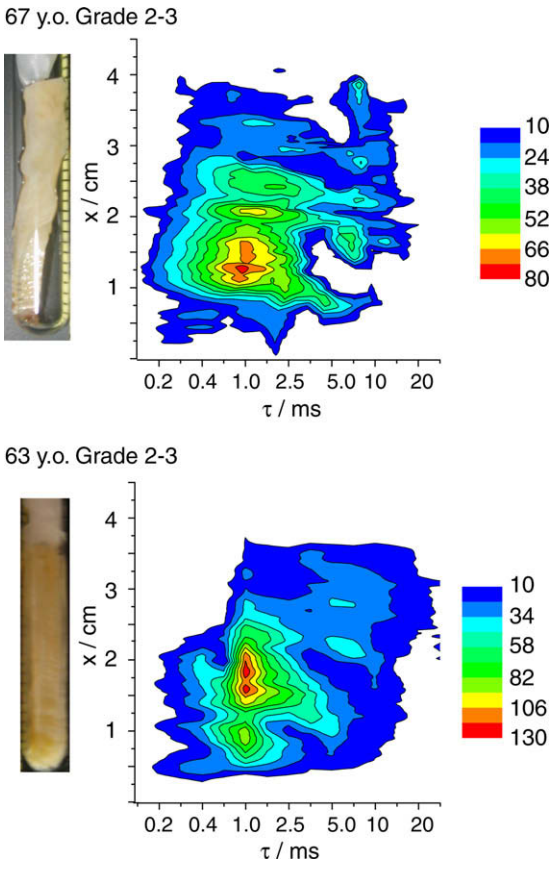

Fig. 3. PITQF τ-maps of two samples of human disc tissue with degenerative grades 2 and 3 (t_{PI} = 1.5 ms). The samples are cores taken from the side of the discs. The top of the sample is from the nucleus pulposus while the bottom is from the annulus fibrosus. The pictures of the tissue are aligned with the vertical axis of the plots.

The τ-maps shown in Fig. 3 clearly display this trend. In the lower three quarters of the image, 0.5–2.75 cm, the signal reaches maximum intensity near 1–2 ms. The signal from the nucleus (2.75–3.75 cm), has much lower intensity. For the 67 year old sample, the signal intensity appears to have two maxima, occurring at 1 and 10 ms, while the topmost part of the sample has a maximum only near 10 ms. This may be indicative of the boundary region between the nucleus and the annulus. The 63-year-old sample exhibits a similar feature with a region near 2.5 cm that appears to have two maxima (1 and 7 ms) while the top part of the nucleus yields a maximum near 5–10 ms. These τ-maps establish that the PITQF imaging technique is effective at distinguishing different parts of the spinal disc tissue based on the ^{23}Na signal. With the extension of this experiment to micro-imaging or medical imaging equipment, it is expected that series of TQF images with varying τ can be acquired and used to study spinal discs and potentially diagnose the stage of disc degeneration. A potential complication is the effect of RF inhomogeneity in large samples, the effect of which on DQF and TQF signal intensities has been analyzed by Reddy et al. [29]. TQF is less sensitive to flip-angle variations and it is probable that good-quality TQF images of regions as small as spinal discs can be obtained *in vivo*.

We have demonstrated a new method for acquiring positive intensity signal from ^{23}Na TQF spectroscopy. It has been found that the simple setup and high resulting signal allow spectroscopic images to be collected. When acquired as a function of TQF creation time, images can be obtained which clearly show that different parts of the disc tissues have different MQF behaviors. These results prove that ^{23}Na TQF imaging is feasible and should be applicable to study spinal disc degeneration.

2. Experimental

Samples were obtained by taking a core sample from the side of a human cadaveric intervertebral disc. Two discs were used, one from a 63-year-old and one from a 67-year-old, both had a Thomson grade of 2–3 [26]. The specimens were sealed into a dialysis membrane (6000 MWCO) and immersed in a 0.12 g/ml solution of polyethylene glycol (PEG 20 k) to emulate physiological conditions [8,30]. The samples were removed from the dialysis bags prior to performing NMR measurements and were sealed in a 5 mm quartz NMR tube.

^{23}Na MQF spectroscopy was performed on a Bruker Avance 600 narrow bore spectrometer using a 5 mm broadband triple resonance solution probe equipped with three-axis gradients. Solution $\pi/2$ pulses were calibrated using a 0.5 M solution of NaCl in water and found to be 7.25 μs; the pulse widths were re-optimized on the samples. Spectral widths of 100 kHz were used, and 2048 points were acquired in the time dimension. 1D spectroscopic images were acquired using the sequence shown in Fig. 2 by applying a 10.7 kHz/cm z-gradient along the sample. Thirteen increments were acquired in the τ dimension to create the τ-maps in Fig. 3. Each spectroscopic image was the sum of 5000 scans using a 0.1 s pulse delay. It was found experimentally that the effective range of the RF coil was approximately 1.5 cm. To acquire images of the entire sample, 3–4 cm in length, the sample was systematically moved through the coil in 1.3 cm increments and the resulting spectroscopic images were summed up post-processing. The spectra were processed used 200 kHz exponential line broadening while the images were processed using 500–1000 Hz line broadening.

Acknowledgments

T.P. acknowledges financial support of the National Institutes of Health (P20-17716 under COBRE program, and 2 P20 016472-04 under INBRE program of NCRR). M.M. acknowledges the financial support of the National Football League Charities Organization. K.J.O. thanks the Natural Sciences and Engineering Research Council of Canada for financial support.

References

[1] S.J. Atlas, R.A. Deyo, Evaluating and managing acute low back pain in the primary care setting, J. Gen. Intern. Med. 16 (2001) 120–131.
[2] E.J. Carragee, T.F. Alamin, J.L. Miller, J.M. Carragee, Discographic, MRI and psychosocial determinants of low back pain disability and remission: a prospective study in subjects with benign persistent back pain, Spine J. 5 (2005) 24–35.
[3] J.P.G. Urban, C.P. Winlove, Pathophysiology of the intervertebral disc and the challenges for MRI, J. Magn. Reson. Imag. 25 (2007) 419–432.
[4] T.R. Walsh, J.N. Weinstein, K.F. Spratt, T.R. Lehmann, C. Aprill, H. Sayre, Lumbar discography in normal subjects—a controlled, prospective study, J. Bone Joint Surg. Am. 72A (1990) 1081–1088.
[5] U. Eliav, G. Navon, Analysis of double-quantum-filtered NMR-spectra of ^{23}Na in biological tissues, J. Magn. Reson. Ser. B 103 (1994) 19–29.
[6] E.K. Insko, T.H. Kaufman, J.S. Leigh, R. Reddy, Sodium NMR evaluation of articular cartilage degradation, Magn. Reson. Med. 41 (1999) 30–34.
[7] T. Knubovets, H. Shinar, U. Eliav, G. Navon, A ^{23}Na multiple-quantum-filtered NMR study of the effect of the cytoskeleton conformation on the anisotropic motion of sodium ions in red blood cells, J. Magn. Reson. Ser. B 110 (1996) 16–25.
[8] W. Perea, M. Cannella, J. Yang, A.J. Vega, T. Polenova, M. Marcolongo, ^{2}H double quantum filtering (DQF) NMR spectroscopy of the nucleus pulposus tissues of the intervertebral disc, Magn. Reson. Med. 57 (2007) 990–999.
[9] R. Reddy, L. Bolinger, M. Shinnar, E. Noyszewski, J.S. Leigh, Detection of residual quadrupolar interaction in human skeletal-muscle and brain in vivo via multiple-quantum-filtered sodium NMR spectra, Magn. Reson. Med. 33 (1995) 134–139.
[10] R. Reddy, S.C. Li, E.A. Noyszewski, J.B. Kneeland, J.S. Leigh, In vivo sodium multiple quantum spectroscopy of human articular cartilage, Magn. Reson. Med. 38 (1997) 207–214.
[11] H. Shinar, U. Eliav, G. Navon, Single and multiple quantum NMR relaxation-times of sodium and potassium in red-blood-cells, Isr. J. Chem. 32 (1992) 299–304.
[12] U. Eliav, H. Shinar, G. Navon, The formation of a 2nd-rank tensor in ^{23}Na double-quantum-filtered NMR as an indicator for order in a biological tissue, J. Magn. Reson. 98 (1992) 223–229.
[13] Y. Sharf, U. Eliav, H. Shinar, G. Navon, Detection of anisotropy in cartilage using ^{2}H double-quantum-filtered NMR spectroscopy, J. Magn. Reson. Ser. B 107 (1995) 60–67.
[14] G. Navon, U. Eliav, D.E. Demo, B. Blümich, Study of order and dynamic processes in tendon by NMR and MRI, J. Magn. Reson. Imag. 25 (2007) 362–380.
[15] K.J. Ooms, M. Cannella, A.J. Vega, M. Marcolongo, T. Polenova, The application of ^{23}Na DQF NMR spectroscopy for the study of spinal disc degeneration, Magn. Reson. Med. 60 (2008) 246–252.
[16] J. Choy, W. Ling, A. Jerschow, Selective detection of ordered sodium signals via the central transition, J. Magn. Reson. 180 (2006) 105–109.
[17] R. Kemp-Harper, S.P. Brown, C.E. Hughes, P. Styles, S. Wimperis, ^{23}Na NMR methods for selective observation of sodium ions in ordered environments, Progr. Nucl. Magn. Reson. Spectr. 30 (1997) 157–181.
[18] E.K. Insko, D.B. Clayton, M.A. Elliott, In vivo sodium MR imaging of the intervertebral disk at 4T, Acad. Radiol. 9 (2002) 800–804.
[19] E. Sulyok, Physical water compartments: a revised concept of perinatal body water physiology, Physiol. Res. 55 (2006) 133–138.
[20] D.E. Woessner, N. Bansal, Temporal characteristics of NMR signals from spin 3/2 nuclei of incompletely disordered systems, J. Magn. Reson. 133 (1998) 21–35.
[21] C.-W. Chung, S. Wimperis, Optimum detection of spin-3/2 biexponential relaxation using multiple-quantum filtration techniques, J. Magn. Reson. 88 (1990) 440–447.
[22] U. Eliav, G. Navon, A study of dipolar interactions and dynamic processes of water molecules in tendon by ^{1}H and ^{2}H homonuclear and heteronuclear multiple-quantum-filtered NMR spectroscopy, J. Magn. Reson. 137 (1999) 295–310.
[23] K. Keinan-Adamsky, H. Shinar, G. Navon, The effect of decalcification on the microstructure of articular cartilage assessed by ^{2}H double quantum filtered spectroscopic MRI, Magn. Reson. Mater. Phys. Biol. Med. 18 (2005) 231–237.
[24] K. Keinan-Adamsky, H. Shinar, G. Navon, Multinuclear NMR and MRI studies of the maturation of pig articular cartilage, Magn. Reson. Med. 55 (2006) 532–540.
[25] A. Borthakur, E.M. Shapiro, J. Beers, S. Kudchodkar, J.B. Kneeland, R. Reddy, Effect of IL-1 beta-induced macromolecular depletion on residual quadrupolar interaction in articular cartilage, J. Magn. Reson. Imag. 15 (2002) 315–323.
[26] J.P. Thompson, R.H. Pearce, M.T. Schechter, M.E. Adams, I.K.Y. Tsang, P.B. Bishop, Preliminary evaluation of a scheme for grading the gross morphology of the human intervertebral-disk, Spine 15 (1990) 411–415.
[27] Y. Seo, K. Ikoma, H. Takamiya, Y. Kusaka, L. Tsoref, U. Eliav, H. Shinar, G. Navon, ^{1}H double-quantum-filtered MR imaging as a new tool for assessment of healing of the ruptured Achilles tendon, Magn. Reson. Med. 42 (1999) 884–889.
[28] L. Tsoref, U. Eliav, Y. Seo, H. Shinar, G. Navon, Slice-selective proton double quantum filtered MRI of joint connective tissues, J. Magn. Reson. Imag. 11 (2000) 336–341.
[29] R. Reddy, M. Shinnar, Z. Wang, J.S. Leigh, Multiple-quantum filters of spin-3/2 with pulses of arbitrary flip angle, J. Magn. Reson. Ser. B 104 (1994) 148–152.
[30] J.P.G. Urban, J.F. Mcmullin, Swelling pressure of the lumbar intervertebral disks—influence of age, spinal level, composition, and degeneration, Spine 13 (1988) 179–187.